doi:10.1093/brain/aws242 Brain 2012: 135; 2938–2951 | 2938

BRAIN
A JOURNAL OF NEUROLOGY

A combined post-mortem magnetic resonance imaging and quantitative histological study of multiple sclerosis pathology

James Kolasinski,[1,2,3]* Charlotte J. Stagg,[1,2]* Steven A. Chance,[2] Gabriele C. DeLuca,[2] Margaret M. Esiri,[2] Eun-Hyuk Chang,[1,2] Jacqueline A. Palace,[2] Jennifer A. McNab,[3] Mark Jenkinson,[1] Karla L. Miller[1] and Heidi Johansen-Berg[1,2]

1 Centre for Functional Magnetic Resonance Imaging of the Brain (FMRIB), University of Oxford, Oxford, OX3 9DU, UK
2 Nuffield Department of Clinical Neurosciences, University of Oxford, Oxford, OX3 9DU, UK
3 Athinoula A. Martinos Centre for Biomedical Imaging, Harvard Medical School, Massachusetts General Hospital, Boston, USA

*These authors contributed equally to this work.

Correspondence to: Dr. Charlotte Stagg,
Centre for Functional Magnetic Resonance Imaging of the Brain,
John Radcliffe Hospital,
Headington, Oxford,
OX3 9DU UK
E-mail: cstagg@fmrib.ox.ac.uk

Multiple sclerosis is a chronic inflammatory neurological condition characterized by focal and diffuse neurodegeneration and demyelination throughout the central nervous system. Factors influencing the progression of pathology are poorly understood. One hypothesis is that anatomical connectivity influences the spread of neurodegeneration. This predicts that measures of neurodegeneration will correlate most strongly between interconnected structures. However, such patterns have been difficult to quantify through post-mortem neuropathology or *in vivo* scanning alone. In this study, we used the complementary approaches of whole brain post-mortem magnetic resonance imaging and quantitative histology to assess patterns of multiple sclerosis pathology. Two thalamo-cortical projection systems were considered based on their distinct neuroanatomy and their documented involvement in multiple sclerosis: lateral geniculate nucleus to primary visual cortex and mediodorsal nucleus of the thalamus to prefrontal cortex. Within the anatomically distinct thalamo-cortical projection systems, magnetic resonance imaging derived cortical thickness was correlated significantly with both a measure of myelination in the connected tract and a measure of connected thalamic nucleus cell density. Such correlations did not exist between these markers of neurodegeneration across different thalamo-cortical systems. Magnetic resonance imaging lesion analysis depicted clearly demarcated subcortical lesions impinging on the white matter tracts of interest; however, quantitation of the extent of lesion-tract overlap failed to demonstrate any appreciable association with the severity of markers of diffuse pathology within each thalamo-cortical projection system. Diffusion-weighted magnetic resonance imaging metrics in both white matter tracts were correlated significantly with a histologically derived measure of tract myelination. These data demonstrate for the first time the relevance of functional anatomical connectivity to the spread of multiple sclerosis pathology in a 'tract-specific' pattern. Furthermore, the persisting relationship between metrics from post-mortem diffusion-weighted magnetic resonance imaging and histological measures from fixed tissue further validates the potential of imaging for future neuropathological studies.

Keywords: multiple sclerosis; post-mortem imaging; diffusion imaging; white matter tracts; neurodegeneration

Received February 6, 2012. Revised June 29, 2012. Accepted July 20, 2012

Abbreviations: LGN-V1 = the thalamo-cortical projection system between the lateral geniculate nucleus and primary visual cortex (optic radiations); MDT-PFC = the thalamo-cortical projection system between the mediodorsal nucleus of the thalamus and prefrontal cortex (component of the anterior thalamic radiations)

Introduction

Multiple sclerosis is a chronic inflammatory demyelinating condition affecting the brain and spinal cord (Compston and Coles, 2008). Despite being the most prevalent disabling adult neurological diagnosis in Europe and North America (Dua *et al*., 2008), our understanding of the cause, pathogenesis and pathophysiology of the condition is incomplete (Stadelmann, 2011), and no treatments are currently available that arrest disease progression (Lopez-Diego and Weiner, 2008). A greater understanding of multiple sclerosis pathology is necessary to allow more effective disease management and therapeutic intervention, yielding improved patient outcomes.

Most early studies into multiple sclerosis focused on the most striking feature of the disease, that of focal white matter demyelination; typically associating disease severity with the spatio-temporal dissemination of sclerotic CNS lesions (Carswell, 1838; Charcot, 1868; McDonald *et al*., 2001; Polman *et al*., 2005). Although such focal demyelination is a well-established feature in multiple sclerosis (Fog, 1950; Brownell and Hughes, 1962), recent studies have strongly implicated a more global underlying inflammatory neurodegeneration (Chard and Miller, 2009) and highlighted the presence of more subtle pathological processes in multiple sclerosis beyond focal plaque formation.

A number of studies have recognized more subtle grey matter and white matter changes in addition to the white matter lesions visible upon gross analysis (Evangelou *et al*., 2000*b*; Geurts and Barkhof, 2008). Cortical atrophy is evident from an early stage, presenting in patients with radiologically isolated syndrome (Amato *et al*., 2012), clinically isolated syndrome (Dalton, 2004) and early in relapsing remitting multiple sclerosis (Chard *et al*., 2002). Post-mortem studies have also revealed diffuse changes in myelination occurring in non-lesional, apparently normal-appearing white matter (Barbosa *et al*., 1994; Kutzelnigg *et al*., 2005; Mistry *et al*., 2011) and grey matter (Bø *et al*., 2003; Gilmore *et al*., 2009), as well as evidence for suboptimal remyelination in the majority of chronic white matter lesions (Albert *et al*., 2007). Extensive axonal damage has been demonstrated in acute white matter lesions and normal-appearing white matter in the progressive stage of the disease, with anatomically associated grey matter demyelination and neuroapoptosis (Ferguson *et al*., 1997; Evangelou *et al*., 2000*b*; Peterson *et al*., 2001). Neuronal loss in cortical and thalamic structures has also been reported in both relapsing remitting multiple sclerosis and progressive multiple sclerosis (Cifelli *et al*., 2002; Wylezinska *et al*., 2003; Wegner, 2006).

These observations suggest an interplay between inflammatory demyelination and remyelination, ongoing axonal damage and neurodegeneration (Evangelou *et al*., 2000*b*; Albert *et al*., 2007; Frischer *et al*., 2009). Such findings have prompted a reappraisal of the spread of multiple sclerosis pathology, the contribution of lesions and the tissues impacted therein. However, currently too little is known regarding the patterns in these varying pathological processes, understanding of which could potentially explain the heterogeneous clinical profile of the disease (Lassmann *et al*., 2001; Weiner, 2009).

Investigating the association between the varying forms of neuropathology in multiple sclerosis has proved difficult. Studies of either neurohistology or MRI-derived data in individual white matter pathways have suggested that neuronal loss in multiple sclerosis can occur by Wallerian or trans-synaptic degeneration of axons damaged by acute white matter lesions (Evangelou *et al*., 2000*a*; Simon *et al*., 2000). Observations of early atrophy in regions of extensive connectivity such as the thalamus and other deep grey matter structures also support a mechanism by which pathology might propagate through connected structures (Henry *et al*., 2008). Whilst previous diffusion-weighted MRI studies have observed apparent structural damage in non-lesional white matter adjacent to multiple sclerosis lesions (Werring *et al*., 2000), assessment of similar connectivity-driven effects in tract systems with more distant associated white matter and grey matter structures has been challenging.

Diffusion-weighted MRI offers sensitive measures of white matter tract integrity and connectivity. This method measures the average distance water molecules displace during a period of time, and the signal thus reflects the constraints and directionality imposed on water movement by the orientation of white matter fibre bundles, their myelin and axonal structures (Beaulieu, 2002). By measuring this diffusive motion along multiple directions, it is possible to calculate metrics such as mean diffusivity and fractional anisotropy. Mean diffusivity quantifies the mean apparent diffusion independent of direction, while fractional anisotropy indicates the degree of diffusion directionality and varies from zero (equal in all directions) to one (movement completely restricted except along one direction). Anisotropic diffusion in white matter has been shown to primarily reflect 'the dense packing of axons and their inherent axonal membrane' (Beaulieu, 2002), and a decrease in fractional anisotropy is therefore commonly held to reflect a reduction in white matter tract integrity. In the study of multiple sclerosis, white matter diffusion-weighted MRI metrics have been shown to correlate strongly with clinical features such as cognitive and visual impairment (Ciccarelli *et al*., 2005; Rocca *et al*., 2007; Dineen *et al*., 2009). A recent assessment of the corticospinal tract and motor cortex in multiple sclerosis using diffusion-weighted MRI has demonstrated an inverse relationship between tract integrity and cortical volume (Gorgoraptis *et al*., 2010). However, *in vivo* studies are limited by the lack of histological correlates for the diffusion-weighted MRI metrics and the assumption that relationships between tissue microstructure and diffusion-weighted MRI metrics persist in complex neuropathology.

In order to assess patterns of diffuse neurodegeneration in multiple sclerosis, we used novel post-mortem whole brain

diffusion-weighted and structural MRI in combination with quantitative histology. We considered two white matter tracts and their associated cortical and thalamic structures based on their distinct neuroanatomy and on their documented involvement in multiple sclerosis: the optic radiations between the lateral geniculate nucleus and primary visual cortex (hereafter LGN-V1) and the component of the anterior thalamic radiations between the mediodorsal nucleus of the thalamus and prefrontal cortex, hereafter MDT-PFC (Ciccarelli *et al*., 2005; Rocca *et al*., 2007; Dineen *et al*., 2009). Our primary aim was to test for associations between markers of diffuse neurodegeneration in the tracts and their associated grey matter structures. Specifically, we hypothesized that measures of diffuse neurodegeneration are more strongly correlated in interconnected grey matter structures and their white matter pathways, than in unconnected structures. In addition, we sought to assess the potential association between subcortical white matter lesion load and patterns of diffuse degeneration in the specific tract systems under study. Our secondary aim was to investigate correlations in post-mortem diffusion-weighted MRI metrics and quantitative histology. We predicted that associations between fractional anisotropy, mean diffusivity and quantitative histological metrics of white matter integrity would persist *ex vivo* in the presence of neuropathology as they do *in vivo* in healthy tissue (Beaulieu, 2002).

Materials and methods

Patients and samples

This study was performed using nine fixed whole brains from patients with a diagnosis of multiple sclerosis, obtained from the UK MS Tissue Bank (Imperial College, Hammersmith Hospital Campus, London) (Table 1). Samples were immersion fixed and stored in 10% neutral buffered formalin. During MRI, brains were placed in perfluoropolyether (PFPE) (Fomblin® LC08; Solvay Inc.). This proton-free fluid medium produces minimal magnetic resonance signal and approximately matches the magnetic susceptibility of tissue, reducing scan artefact, particularly at the exposed pial surface in *ex cranio* post-mortem samples (Alper *et al*., 1980; Forster *et al*., 1991; Ziegler *et al*., 2011). For an overview of the tissue processing and analysis, see Fig. 1.

Magnetic resonance imaging

All scanning was undertaken on a Siemens Trio 3 T scanner in a standard 12-channel head coil. The total experiment time for each sample was ~24 h. In each case, three averages of diffusion-weighted data were acquired using a 3D-segmented echo planar imaging sequence (echo time/repetition time = 122/530 ms, bandwidth = 789 Hz/pixel, matrix size: 168 × 192 × 120, resolution 0.94 × 0.94 × 0.94 mm). Diffusion weighting was isotropically distributed along 54 directions (b = 4500 s/mm^2) with six $b = 0$ images for a total scan time of ~6 h per average. Structural data were acquired using a 3D balanced steady-state-free precession sequence with radio frequency phase alternation to avoid banding artefact (echo time/repetition time = 3.7/7.4 ms, bandwidth = 302 Hz/pixel, matrix size: 352 × 330 × 416, resolution 0.5 × 0.5 × 0.5 mm) repeated eight times and averaged to increase signal to noise ratio. More details of the protocol have been published previously (Miller *et al*., 2011).

All magnetic resonance data were processed using components of the FMRIB software library (FSL) (Smith *et al*., 2004; Woolrich *et al*., 2009). Diffusion-weighted MRI data were processed using the FSL diffusion toolbox (FDT) (Behrens *et al*. 2003*a*) with a pipeline developed in-house to compensate for gradient-induced-heating drift and eddy-current distortions, to give maps of fractional anisotropy, mean diffusivity and principle diffusion vectors (Miller *et al*., 2011).

Multi-fibre probabilistic tractography was performed (ProbtrackX, FDT) (Behrens *et al*., 2007) in order to define the white matter tracts of interest. We chose not to perform tractography in the multiple sclerosis brains as the presence of extensive pathology, along with the low signal to noise ratio of post-mortem diffusion data, results in highly variable tracking performance that can be challenging to interpret. Tracking was therefore undertaken using *in vivo* data previously acquired from nine healthy control subjects. Control diffusion-weighted MRI data were acquired on a Siemens Sonata 1.5 T scanner at the Oxford Centre for Magnetic Resonance, Oxford, UK, with a maximum gradient strength of 40 mT/m. Three sets of echo-planar images of the whole head were acquired. Diffusion weighting was isotropically distributed along 60 directions ($b = 1000$ s/mm^2) with nine $b = 0$ images. 72 × 2-mm thick axial slices were acquired, giving an isotropic resolution of 2 × 2 × 2 mm. *In vivo* control data were age matched to the post-mortem multiple sclerosis cohort as far as possible, to within a maximum of 4 years.

Tractography was undertaken using thalamic seed masks and cortical way-point masks to assess the LGN-V1 and MDT-PFC tracts, respectively. Anatomically defined thalamic and cortical masks were manually created on a standard space template prior to registration

Table 1 Subject demographics

Subject ID	Sex	Age (years)	Disease progression	Disease duration (years)	Post-mortem interval (h)	Scan interval (days)	Cause of death
1	F	69	2°	37	66	1198	Multiple sclerosis
2	F	74	1°	33	40	929	Sepsis
3	F	78	2°	45	60	435	Colonic carcinoma
4	F	79	2°	55	26	1052	Pneumonia
5	M	72	2°	28	59	1201	Pneumonia
6	F	50	2°	22	69	1134	Breast cancer (metastasized)
7	M	66	2°	15	37	1126	Prostate cancer
8	F	86	1°	54	54	578	Lymphoma
9	F	60	2°	11	21	539	Multiple sclerosis

1° = primary progressive; 2° = secondary progressive; F = female; M = male.

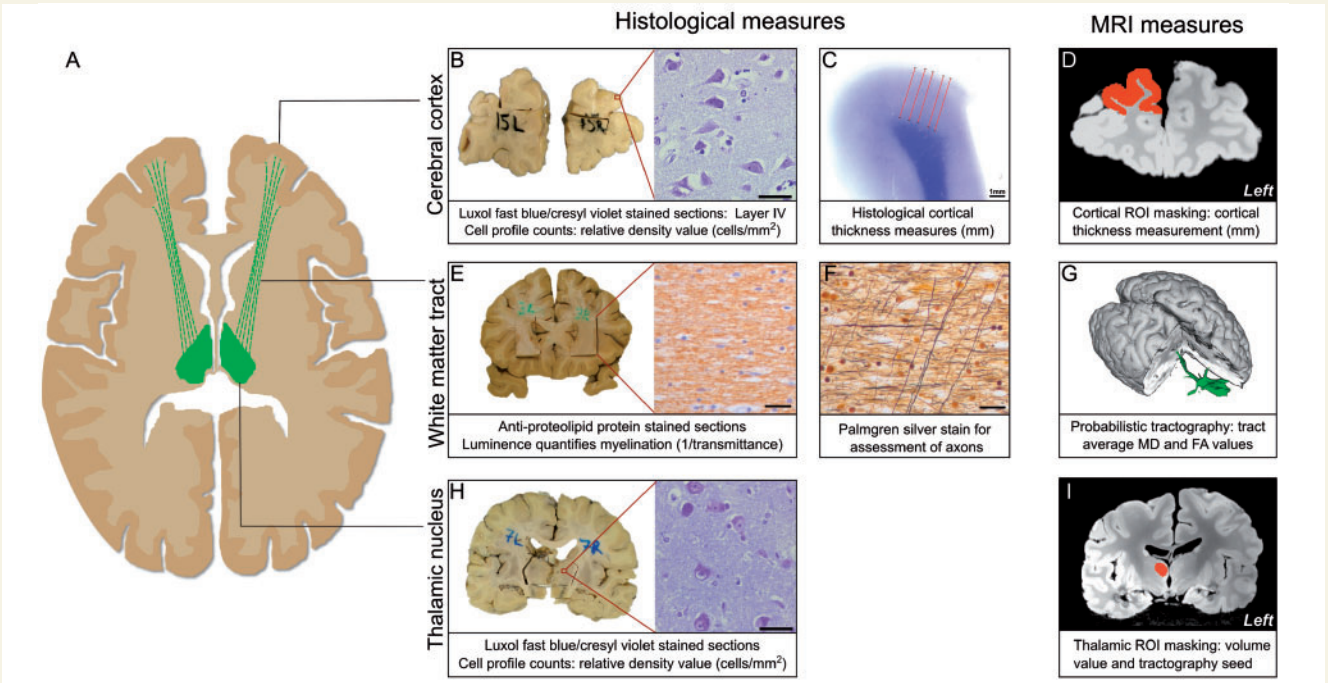

Figure 1 Overview of imaging and histological analysis of non-lesional brain tissue. Brains were scanned and subsequently sampled histologically to assess markers of neuropathology along the tract running from the mediodorsal nucleus of the thalamus to the prefrontal cortex (**A**, green) and from the lateral geniculate nucleus of the thalamus to the visual cortex (not shown). MRI provided structural images (**D** and **I**) and diffusion-weighted data yielding mean diffusivity (MD) and fractional anisotropy (FA) maps. Histological sampling of grey matter structures [example sampled blocks from prefrontal cortex (**B**) and mediodorsal nucleus of the thalamus (**H**) shown for illustration; V1 and lateral geniculate nucleus were also sampled] was followed by manual neuronal/glial profile counts on Luxol fast blue/cresyl violet sections (**B** and **H**). MRI cortical thickness masking was undertaken on MRI in regions analogous to histological samples (**B** and **D**: corresponding regions for prefrontal cortex); values were validated using histological measures (**C**). The grey matter structures sampled histologically were masked in their entirety in standard structural MRI space and used as the basis for probabilistic tractography of the tracts of interest in control *in vivo* brains. Paired thalamic and cortical masks were used as start points (seed masks) and end points (target masks), respectively to yield tractography outputs (**G**: 3D MDT-PFC tract shown in green), which were transformed using affine registration into the post-mortem image diffusion space. The resulting tract regions of interest (ROI) were used to derive average tract diffusion metrics, excluding regions of lesion-tract overlap. Registered tractography outputs guided histological sampling of white matter blocks corresponding to the tract midpoint (**E**). White matter sections were stained with anti-proteolipid protein stain (**E**: brown, myelin) and assessed for light transmittance (T) in regions corresponding to the tract (defined in G) to quantify myelin content (1/T). Adjacent white matter sections were stained with Palmgren silver to assess for axonal pathology in the tract using a point counting method (**F**). Scale bars: **B** and **H** = 80 μm; **E** and **F** = 25 μm.

into the respective *in vivo* control diffusion spaces, with reference to the Oxford Thalamic Connectivity Atlas (Behrens *et al*., 2003*a*, *b*; Johansen-Berg *et al*., 2005), the Harvard–Oxford Subcortical Structural Atlas (Frazier *et al*., 2005) and neuroanatomical atlases (DeArmond *et al*., 1989; Hirai *et al*., 1989). Masks representing the prefrontal cortex and primary visual cortex were produced with specific reference to anatomical definitions commonly accepted in previous magnetic resonance studies (Stensaas *et al*., 1974; Wible *et al*., 1995).

During probabilistic tractography, repetitive sampling from the seed mask region of interest computed potential streamlines through local samples to reconstruct a tract based on voxel-wise distribution of principle diffusion directions (5000 streamlines/seed voxel, loop check activated). Only streamlines that passed from the respective paired thalamic region of interest mask to the ipsilateral cortical region of interest mask were included in the output. Derived tracts were highly comparable to atlas tracts from the John Hopkins Universtiy white-matter tractography atlas (Hua *et al.*, 2008) (Supplementary Fig. 1). The derived standard space tracts were thresholded to include only those present in at least three of nine control subjects, binarized and transferred into both the structural and diffusion space of the individual post-mortem brains using affine registration (FSL Linear Registration Tool: FLIRT) (Fig. 2). Mean values of fractional anisotropy and mean diffusivity in non-lesional tract white matter were acquired for each tract region of interest from the corresponding region of the diffusion space of each post-mortem multiple sclerosis brain, excluding regions overlapping with lesion masks (Supplementary Fig. 2C and D).

Cortical regions of interest were masked on the structural post-mortem images as regions corresponding to those sampled histologically, defined using photographic images of coronal 10-mm slices recorded before and after the region of interest tissue block was removed. MRI cortical thickness in these regions of interest (Fig. 1D) was subsequently determined using in-house scripts using the FSL distancemap function (Smith *et al*., 2006) to compute an average thickness value, taking as input the manual delineation of the grey matter/white matter boundary and cortical surface. The MRI acquisition parameters required for post-mortem scanning and changes to MRI tissue parameters with death and fixation made more automated approaches unreliable.

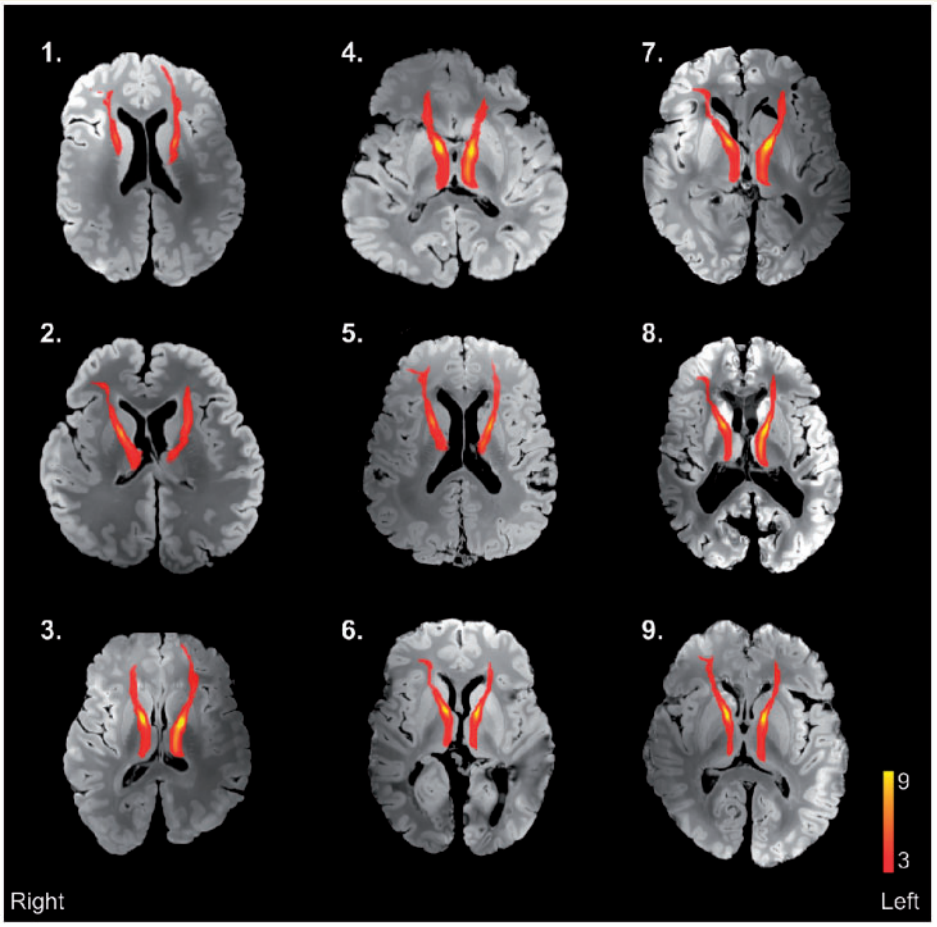

Figure 2 Results of control mediodorsal nucleus of the thalamus-prefrontal cortex tract output registration into structural space of individual post-mortem MRI scans of multiple sclerosis brains. Structural images were obtained using a balanced steady-state-free precession sequence. Tracts have been thresholded to display only those present in ⩾ 3/9 control subjects. Case numbering corresponds to Table 1.

Neurohistological sampling

All brains were sectioned coronally and examined by a clinical neuropathologist to confirm a diagnosis of multiple sclerosis and to assess for additional pathology. Blocks of 25 × 25 × 10 mm were sampled bilaterally from the anatomically defined cortical and thalamic regions of interest (Fig. 1B and H) documented using a C4040 digital camera (Olympus). During the sampling of each individual brain, the corresponding structural magnetic resonance images and individual tractography results were consulted in the cutting room on a laptop computer. In order to ensure that cortical samples were taken from regions of the cortex subserved by the relevant white matter tract, cortical sampling was guided by both the tractography results and previous connectivity studies (Behrens *et al.*, 2003*b*). Prefrontal cortex blocks incorporated the middle and superior frontal gyri with an inferior boundary medially at the paracingulate sulcus and laterally superior to the inferior frontal sulcus, in line antero-posteriorly with the frontal genu of the cingulate. V1 blocks were sampled at the banks of the calcarine fissure in line antero-posteriorly with the medium transverse occipital gyrus. Gross abnormalities were avoided, though in practice this did not alter sampling of any brain under study.

Thalamo-cortical white matter was sampled consistently in a single 10 mm block at the midpoint between the thalamic and cortical regions of interest to ensure consistent histological sampling from each tract system (Fig. 1E and G). The decision to sample at the tract midpoint aimed to maximize the likelihood of observing any trans-synaptic effects propagating from either the thalamic nuclei or the cortex. Sampling was guided by the tractography results, ensuring blocks were consistently cut at an MRI-defined point approximately equidistant between mediodorsal nucleus of the thalamus and prefrontal cortex, and lateral geniculate nucleus and V1. No sampled block or assessed section contained lesions at a macroscopic or microscopic level.

Tissue blocks were embedded in paraffin wax, sectioned at 10 μm, and serial sections were stained with Luxol fast blue (Alfa Aesar) and cresyl violet (ThermoFisher Scientific) for cell density analysis (Fig. 1B and H), anti-proteolipid protein stain (AbD AbSerotec) (anti-proteolipid protein) (Fig. 1E) for light transmittance myelin quantification and Palmgren silver to visualize axons (Fig. 1F).

Cell density analysis

Cell profile counting was undertaken in all grey matter regions of interest on a section selected from the middle of each block using KS400 v.3.0 image analysis software (Carl Zeiss) on a PC receiving a signal from a KY-F30 3CCD video camera (JVC) mounted on a BH-2

microscope (Olympus Optical) with a ×40 objective lens. A counting frame of 90 × 90 μm was superimposed over the images. The bottom and left borders formed exclusion planes. In cortical regions of interest, cells in layer IV were counted; both pyramidal and non-pyramidal neurons were counted together and could be clearly distinguished from glia on Luxol fast blue/cresyl violet sections by the presence of Nissl substance and a visible nucleolus. Profile counting was undertaken in 25 frames within an optically defined anatomical region of interest using systematically random sampling in each section: the counting frame was moved in a 2D raster pattern of defined step lengths in the *x* and *y* directions using the vernier scale beginning at a random position with respect to the boundaries of the region of interest (Evangelou *et al*., 2001).

Histological cortical thickness analysis

In order to validate and complement MRI-derived cortical thickness measures, histological measures of cortical thickness were taken in cortical regions of interest from Luxol fast blue/cresyl violet stained sections as described previously (Pomeroy *et al.*, 2008) (Supplementary Fig. 3A) using ImageJ (US National Institutes of Health).

Cerebral white matter analysis

All assessment of tract white matter was undertaken using Axiovision v4.7.2 software on a PC receiving a signal from an Axiocam MRc (Carl-Zeiss) mounted on a BX40 microscope (Olympus. Japan) with a ×40 objective lens unless otherwise stated.

Myelin content in tract white matter samples was assessed using light transmittance to quantify the intensity of the myelin stain in anti-proteolipid protein-stained sections (Fig. 1E). No sampled blocks or assessed sections contained lesions at a macroscopic or microscopic level. The set-up was calibrated in RGB mode with fixed white balance and incident light, using a standard slide/coverslip preparation and light filters (6% and 25% transmittance) to calculate a linear regression ($R^2 = 1.00$) between the camera-defined densitometric light intensity and corresponding percentage maximum light transmittance (T). Five measures of maximum light transmittance were taken in a tractography-defined tract cross-section region of interest using a 150 × 150 μm virtual frame on anti-proteolipid protein stained sections. The resulting values were averaged. Data are presented as 1/T for intuitive analysis: greater light impedance suggests higher myelin content.

Overt axonal pathology in non-lesional white matter was initially assessed qualitatively using Palmgren silver in sections adjacent in the tissue block to those used for myelin transmittance analysis. In order to quantify whether more subtle axonal pathology was present in non-lesional white matter, and its potential contribution to any observed variation in the level of non-lesional white matter myelination, a relative measure of axonal density was derived from the Palmgren silver-stained sections using a point sampling method. In line with previous applications of this technique in the study of multiple sclerosis (Dziedzic *et al.*, 2010), we assessed 10 microscopic fields in each white matter tract region of interest with a ×60 objective lens and a digitally overlaid 25-point Chalkey array. The number of array points crossed by one or more axons was expressed as a percentage of the total number of array points, providing a measure of relative axonal density (Supplementary Fig. 4). Stained axons that were clearly continuous, in or out of the plane of view, were counted only once. Axons passing at a tangent, but not crossing a given array point, were not counted.

Lesion labelling and analysis

Lesion masking was undertaken on T_2-weighted B0 volumes acquired during diffusion-weighted MRI sequences. Lesions were identified as regions of well-defined hyperintense signal, as previously described in post-mortem multiple sclerosis tissue (De Groot *et al.*, 2001). Subcortical white matter lesions were manually segmented with individual labels (Supplementary Fig. 2A and B) under the guidance of a clinical neurologist. The resulting lesion masks were assessed in all three orthogonal planes. Whole-brain lesion load was calculated, correcting for brain volume (Supplementary Table 1). Proportional tract lesion load was determined for each individual tract as the volume overlap between the lesion mask in a certain individual, and the volume of a specific tract mask for that individual, expressed as a percentage of overall tract volume (Supplementary Fig. 2C and D).

Statistical methods

The normality of all data used in parametric correlative analysis was confirmed using Shapiro–Wilk tests. Our primary measures were MRI-derived cortical thickness, intensity of myelin staining in non-lesional tract white matter, and a measure of thalamic nucleus cell density. Pearson's coefficient (one-tailed, $P < 0.05$ significant) was used in partial correlations to explore intra- and inter-tract associations between markers of diffuse neuropathology. All inter/intra-tract correlation analysis was corrected for the age of the subject at the time of death and the post-mortem interval between death and fixation (post-mortem interval), as these have previously been shown to have significant effects on diffusion-weighted MRI metrics (D'Arceuil and de Crespigny, 2007; Miller *et al*., 2011). To test the hypothesis that measures of neurodegeneration correlate within tracts but not between tracts, we used distinct procedures to detect any significant (unpredicted) inter-tract associations and to ensure consistent (predicted) intra-tract associations. Specifically, we used a conjunction test over all intra-tract associations and an omnibus test over all inter-tract associations (Nichols *et al*., 2005). The conjunction test considered the maximum *P*-value across intra-tract correlations. In this stringent analysis, the compound null hypothesis can only be disproved if all of the intra-tract associations are significant. The omnibus test considered the minimum *P*-value across all inter-tract associations. While one can never prove the null hypothesis, this liberal test should give good power to detect any possible inter-tract associations.

While our primary tests were performed using MRI-derived measures of cortical thickness, our preferred measure of cortical neurodegeneration, further exploratory analyses were performed to test whether patterns of association were similar if histological measures of cortical thickness or cortical layer IV cell counts were used to quantify cortical neurodegeneration. These tests were performed using Pearson's coefficient (one-tailed, $P < 0.05$ significant) in partial correlations, correcting for post-mortem interval and age.

Associations between tract lesion load and measures of diffuse neurodegeneration within the thalamo-cortical projection systems were assessed using Spearman's rank order correlation (one-tailed, $P < 0.05$ significant). The associations between cortical thickness values derived from MRI and histological methods, and between myelin transmittance values and relative axonal density, were assessed using Pearson's coefficient (one-tailed, $P < 0.05$ significant) in bivariate correlations.

To assess the relationship between quantitative histological measures of myelination and diffusion MRI metrics from white matter tract regions, Pearson's coefficient (one-tailed, $P < 0.05$ significant) was used in partial correlations, correcting for post-mortem interval and age.

Statistical analysis was undertaken using SPSS v.19.0.1 (IBM). Missing values were excluded pairwise. Histological and imaging data are presented in Supplementary Table 1.

Results

Cortical thickness validation

To assess the concurrence of cortical thickness measures derived from MRI and more traditional histological measurements, we performed correlative analysis on measures derived from equivalent cortical regions of interest from the two modalities. Overall, there was a significant correlation between the two metrics ($r = 0.621$, $P \leqslant 0.001$) (Supplementary Fig. 3B), which persisted in the analysis of the measures derived from individual cortical regions of interest (Supplementary Fig. 3C and D).

Intra-tract versus inter-tract patterns of pathology

To assess whether tract-specific patterns of pathology exist within multiple sclerosis, we performed a correlative analysis of markers of neurodegeneration both within and across the two distinct thalamo-cortical projection systems, specifically investigating the relationship between MRI cortical thickness, cell profile density in the thalamic nucleus and the intensity of myelin staining within the connecting tract white matter (Table 2). A conjunction test supported the hypothesis that all intra-tract associations were significant, such that the greater the degeneration in the cortical region, the greater the reduction in myelination in the connected non-lesional tract white matter and the greater the cell loss in the associated thalamic nucleus [(minimum) $r = 0.438$, (maximum) $P = 0.045$; Fig. 3]. By contrast, an omnibus test across all associations of measures between different thalamo-cortical projection systems found no evidence of any significant inter-tract correlations [(minimum) $r = 0.318$, (minimum) $P = 0.115$; Fig. 4].

A similar pattern was observed using histological cortical thickness, once again demonstrating the contrast between positive intra-tract correlations (Supplementary Fig. 5) and absent inter-tract correlations (Supplementary Fig. 6) in all but a single relationship. A summary of the contrast in intra/inter-tract correlations using both MRI and histological cortical thickness is presented in Table 2.

Cell counts from cortical layer IV partially replicated our pattern of positive intra-tract and absent inter-tract correlations. For intra-tract relationships, significant positive correlations were found between layer IV neuronal counts and the intensity of myelin staining in non-lesional tract white matter (LGN-V1: $r = 0.471$, $P = 0.038$; MDT-PFC: $r = 0.591$, $P = 0.013$) (Supplementary Fig. 7A and C), but no such trend was observed between layer IV neuronal counts and a measure of thalamic nucleus cell density (all $P > 0.055$) (Supplementary Fig. 7B and D). All inter-tract relationships were non-significant (all $P > 0.112$) (Supplementary Fig. 8).

Axonal density

In order to assess the relationship between axonal density and diffuse changes in myelination observed in thalamo-cortical non-lesional white matter (Supplementary Fig. 9A and C), we used a point sampling method to gain a quantitative measure of relative axonal density using Palmgren silver in white matter sections adjacent to those used in myelin light transmittance analysis (Supplementary Fig. 9B and D).

Despite the substantial variation in myelin transmittance across the tracts, there was no clear relationship between changes in tract myelination and axonal density (Supplementary Fig. 9E and F). Although it is possible that the detection of subtle relationships between diffuse demyelination and changes in axonal density was beyond the resolution of the applied point sampling method, the current methods were sufficiently robust to detect any overt changes in axonal density and have been applied widely in the field of multiple sclerosis (Brück *et al.*, 1997; Dziedzic *et al.*, 2010). The oblique and non-unified directionality of axonal fibres in the subcortical white matter precluded more detailed quantitative analysis of axonal density in this region as has been previously undertaken in specific tracts of the spinal cord (DeLuca *et al.*, 2004; Tallantyre *et al.*, 2009).

Lesion analysis

Lesion masking across the nine brains under study yielded a range of whole-brain lesion load (Supplementary Table 1), but with a common stereotypical distribution (Supplementary Fig. 2B). There was a predominantly periventricular pattern, ranging from large confluences to small isolated structures, often with perpendicular ovoid extensions from the ventricular border (McAlpine and Compston, 2010; Reimer *et al.*, 2010).

Table 2 Significance of correlations within and between thalamo-cortical systems

		LGN cell density (cells/mm^2)	LGN-V1 tract myelination (1/T)	MDT neuronal density (cells/mm^2)	MDT-PFC tract myelination (1/T)
V1 cortical thickness (mm)	**MRI**	**$r = 0.438$ $P = 0.045$**	**$r = 0.512$ $P = 0.021$**	$r = 0.088$ $P = 0.377$	$r = 0.256$ $P = 0.178$
	Histology	**$r = 0.549$ $P = 0.014$**	**$r = 0.450$ $P = 0.040$**	$r = -0.106$ $P = 0.353$	$r = -0.262$ $P = 0.173$
Prefrontal cortex cortical thickness (mm)	**MRI**	$r = -0.136$ $P = 0.308$	$r = 0.318$ $P = 0.115$	**$r = 0.485$ $P = 0.033$**	**$r = 0.540$ $P = 0.019$**
	Histology	$r = -0.276$ $P = 0.150$	$r = 0.325$ $P = 0.110$	$r = 0.093$ $P = 0.371$	**$r = 0.640$ $P = 0.005$**

An overview of the significance of the correlations observed across the two thalamo-cortical projection systems under study using both MRI and histological cortical thickness values. Values in bold $P < 0.05$; otherwise $P > 0.05$. T = light transmittance. LGN = lateral geniculate nucleus; MDT = mediodorsal nucleus of the thalamus; PFC = prefrontal cortex.

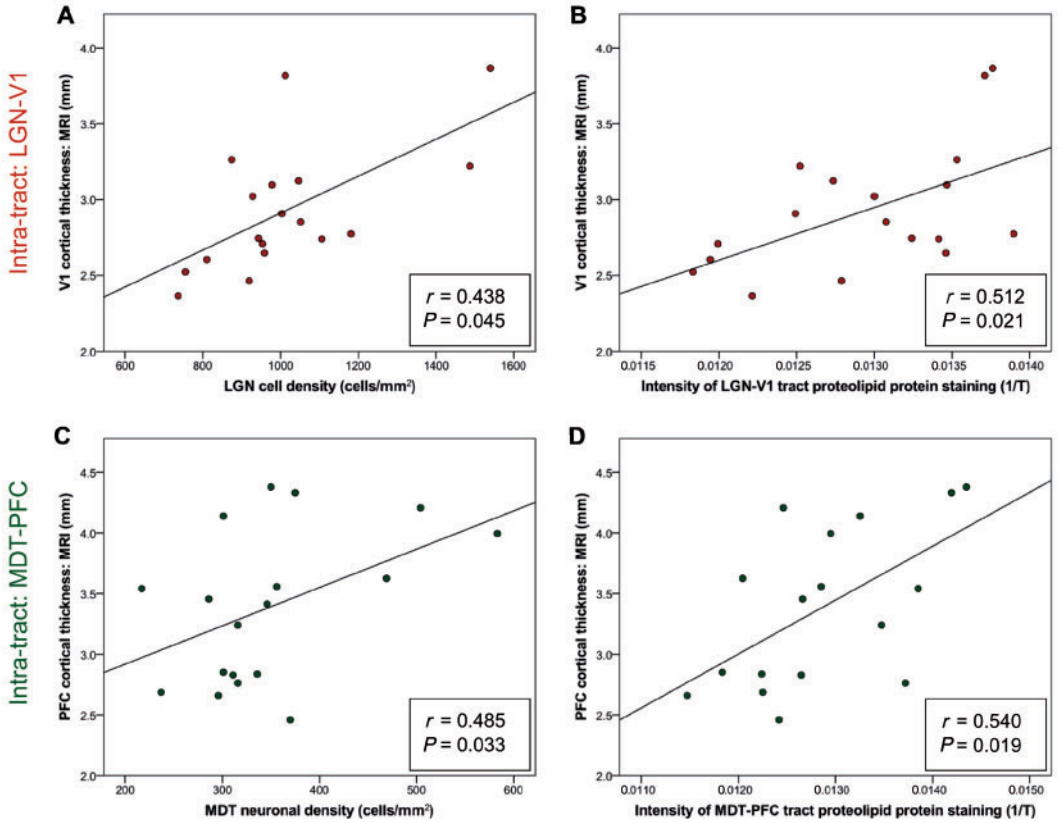

Figure 3 Significant 'intra-tract' correlations between MRI cortical thickness and both (**A** and **C**) a measure of thalamic nucleus cell density and (**B** and **D**) the intensity of staining for proteolipid protein ('level of myelination') in both LGN-V1 and MDT-PFC. T = light transmittance.

Histological assessment of these plaques demonstrated a clear reduction in myelination (Supplementary Fig. 10A, E and I) but considerable variability in axonal density, with some demonstrating minimal axonal disruption and others showing clear loss (Supplementary Fig. 10B, F and J). In order to assess the potential contribution of tract lesion load to patterns of diffuse degenerative processes in the connected tract structures, we assessed the relationships between tract lesion load (percentage of tract disrupted by lesion) (Supplementary Fig. 2C and D) and measures of diffuse pathology throughout the grey matter and white matter structures in the associated tract (Supplementary Fig. 11). Despite the wide range of lesion disruption, particularly from the LGN-PFC tract system, no significant association was observed between increased tract lesion burden and the expected increase in cortical atrophy, cortical layer IV cell loss, diffuse reductions in non-lesional white matter myelination, or cell loss in the associated thalamic nucleus in either tract (Spearman's rank-order coefficient, all $P > 0.099$, data not shown).

Our measures highlight a clear tract-specific relationship between cortical neurodegeneration and diffuse changes in myelination in non-lesional tract white matter. However, a similar relationship is not observed between tract white matter lesion load and the markers of diffuse pathology within the associated thalamo-cortical projection system.

Myelination and post-mortem diffusion metrics

It has previously been suggested that post-mortem diffusion-weighted MRI metrics may not reflect tissue microstructure to the same extent as they do *in vivo* (Shepherd *et al*., 2009*a*, *b*), which may be the source of lower fractional anisotropy and mean diffusivity values in our data compared to that seen *in vivo* (Miller *et al*., 2011). We assessed correlations between the intensity of myelin staining in non-lesional tract white matter quantified through light transmittance analysis and diffusion-weighted MRI metrics in the tracts studied, excluding regions of tract-lesion overlap (Supplementary Fig. 2C and D). The intensity of myelin staining in the white matter tracts was significantly correlated with both tract fractional anisotropy ($r = 0.307$, $P = 0.041$) and tract mean diffusivity ($r = -0.302$, $P = 0.044$) (Fig. 5). Despite global reductions in these parameters, greater tract myelination was associated with higher values of fractional anisotropy and lower values of mean diffusivity.

Discussion

The primary aim of this study was to investigate patterns of diffuse neurodegeneration in multiple sclerosis. Using novel

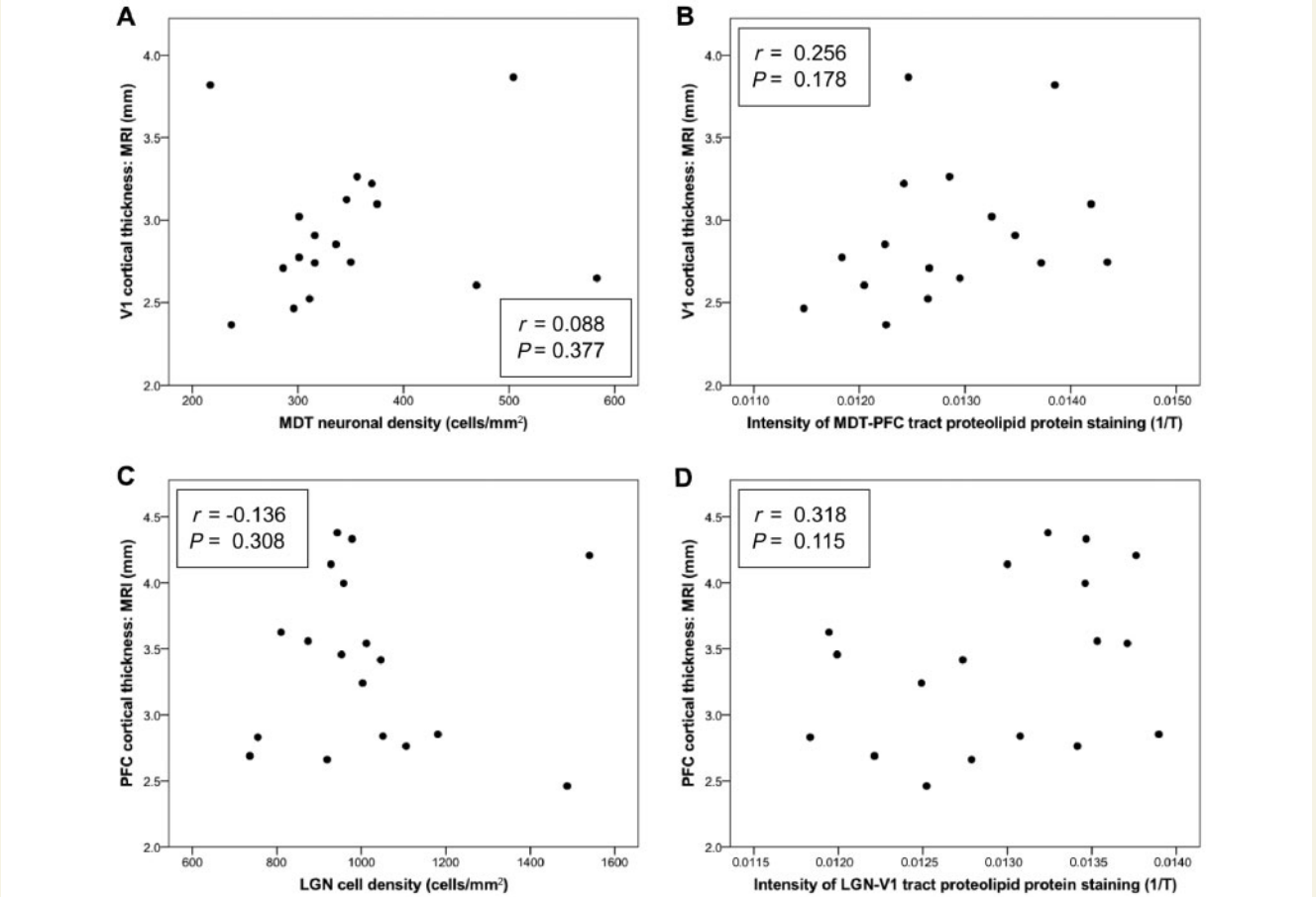

Figure 4 Absence of significant 'inter-tract' correlations between MRI cortical thickness and both (**A** and **C**) a measure of thalamic nucleus cell density and (**B** and **D**) the intensity of staining for proteolipid protein ('level of myelination') in both LGN-V1 and MDT-PFC. T = light transmittance.

post-mortem MRI techniques combined with quantitative histology, we have demonstrated that correlations exist between markers of diffuse neurodegeneration within, but not between, anatomically distinct tracts and grey matter structures in the multiple sclerosis brain. These data provide evidence consistent with the hypothesis that patterns of anatomical connection influence the spread and progression of neurodegeneration in multiple sclerosis. Focal changes in MRI cortical thickness show a clear intra-tract correlation with diffuse changes elsewhere in the associated tract system—a pattern almost completely reproduced using traditional histological metrics of cortical thickness (Supplementary Figs. 5 and 6). The observation that neuronal density in layer IV of the cortical regions of interest partially replicated our pattern of positive intra-tract and absent inter-tract correlations (Supplementary Figs. 7 and 8) was further supportive of some trans-synaptic effect, given that layer IV is traditionally considered a major input for thalamo-cortical afferents from thalamic relay nuclei (Jones, 1998). The patterns observed again suggest that the reduced integrity non-lesional thalamo-cortical tract white matter is associated with neurodegeneration in anatomically connected cortical regions.

The anatomical specificity of our relationships supports the hypothesis that neurodegeneration within multiple sclerosis is driven by a tract-specific process, implying a link between diffuse changes in the myelination of non-lesional white matter and neurodegeneration in anatomically connected regions. These findings are in line with previous studies suggestive of trans-synaptic or Wallerian degeneration in multiple sclerosis (Evangelou *et al.*, 2000*a*; Simon *et al.*, 2000). Axonal staining did not demonstrate any overt pathology in the regions of subcortical non-lesional tract white matter under study (Supplementary Fig. 9), particularly in comparison with that seen in areas with lesions (Supplementary Fig. 10). Measures of relative axonal density derived from point sampling techniques applied in these white matter tracts showed no relationship with measures of tract myelination. Previous studies of multiple sclerosis have reported both trans-synaptic axonal pathology (Dziedzic *et al.*, 2010) and diffuse reductions in myelination in non-lesional white matter (Leary *et al.*, 1999; Kutzelnigg *et al.*, 2005). The lack of any association between diffuse reductions in tract myelin staining and clear concurrent reductions in tract axonal density leads us to speculate that the process observed here is the true loss of myelin, rather than a reduction in myelin levels secondary to axonal loss. Although it is impossible to comment on the temporal dynamics of multiple sclerosis pathology from our data, the results suggest that the diffuse loss of myelin may play a key role in propagating the

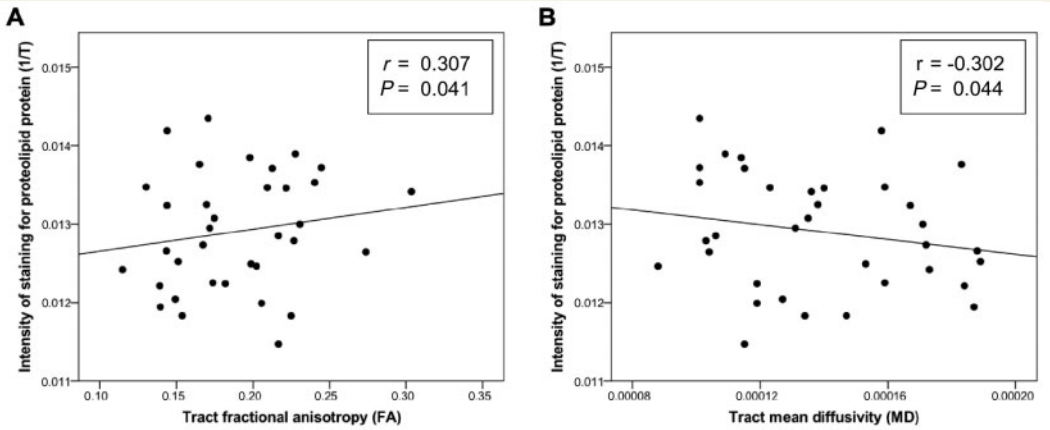

Figure 5 Correlations between intensity of staining for proteolipid protein in non-lesional tract white matter and tractography-derived diffusion-weighted MRI metrics, excluding tract-lesion overlap. Correlations (Pearson's partial correlation coefficient corrected for post-mortem interval and age) between (**A**) tract fractional anisotropy and tract myelin proteolipid protein stain intensity and (**B**) tract mean diffusivity and tract myelin proteolipid protein stain intensity. T = light transmittance.

kind of tract specific patterns in neuropathological markers observed in this study.

The observation of clearly demarcated lesions impinging to a varying extent on the tracts under study (Supplementary Table 1 and Supplementary Fig. 2C and D) provides an opportunity to evaluate the relationship between plaque related pathology and the observed process of diffuse degeneration in the specific thalamo-cortical projection systems. Quantitative analysis of proportional lesion load impinging upon the individual tracts failed to demonstrate any appreciable association between focal lesion load and the severity of neurodegeneration observed therein (Supplementary Fig. 11). This is perhaps unsurprising given the complex and varying relationship between multiple sclerosis lesion load and a range of both pathological and functional metrics of disease severity and progression (Confavreux *et al.*, 2003; DeLuca *et al.*, 2006; Kremenchutzky *et al.*, 2006; Scalfari *et al.*, 2010). Given the patients included in this study were in the late, progressive stage of the disease, the relationship between tract focal lesion load and diffuse tract pathology may be blurred by a plateau earlier in disease: a phenomenon described in a subset of pathological and clinical studies of multiple sclerosis (Li *et al.*, 2006; Sormani *et al.*, 2009; Caramanos *et al.*, 2012). As in a recent study of multiple sclerosis lesion load in the visual pathway and atrophy in the lateral geniculate nucleus (Sepulcre *et al.*, 2009), it is possible that a clearer relationship between tract lesion load and subtle tract pathology may be observed in a more varied patient sample: the biases of post-mortem studies certainly apply here. While it would be favourable to evaluate the relationship between tract lesion load and diffuse neurodegenerative tract pathology across a broad range of patients with relapsing remitting multiple sclerosis and progressive multiple sclerosis, the restricted availability of the post-mortem tissue required to apply the novel imaging/histological approach makes such an investigation unfeasible at present.

Previous evidence for tract-specific associations between changes in myelination and neurodegeneration in multiple sclerosis have been confined mainly to the optic nerves and central visual pathway by virtue of their involvement in optic neuritis. Degeneration in the lateral geniculate nucleus associated with optic nerve dysfunction has been acknowledged for some time (Goldby, 1957), and animal models have demonstrated retrograde degeneration in the optic pathways following tumour necrosis factor alpha-induced optic neuropathy (Madigan, 1996). In multiple sclerosis, histological studies have correlated optic nerve axonal loss with parvocellular atrophy in the lateral geniculate nucleus in humans (Evangelou *et al.*, 2001*b*). MRI studies have associated visual disability in multiple sclerosis optic neuritis with both tractography-defined alterations in optic radiation integrity and structure (Ciccarelli *et al.*, 2005) and magnetization transfer ratio changes in the visual cortex (Audoin *et al.*, 2006). Suggestion of trans-synaptic effects in the mediodorsal nucleus of the thalamus-prefrontal cortex tract has not been documented previously in multiple sclerosis, but there is evidence for correlations between cognitive dysfunction and prefrontal cortex atrophy (Morgen *et al.*, 2006; Portaccio *et al.*, 2006), as well as changes in anterior thalamic radiation integrity on diffusion-weighted MRI (Dineen *et al.*, 2009). The specificity of our correlations supports the notion that connectivity-driven degeneration exists in multiple sclerosis above and beyond the generalized degenerative processes previously reported in the disease (Lindberg *et al.*, 2004).

Our findings concur with previous reports suggesting that focal lesions fall short of explaining the apparent diffuse measures of degeneration evaluated in this study. The driving forces behind these diffuse pathological changes and the robust tract-specific pattern observed are not completely understood but are likely to reflect a complex interplay between chronic inflammation (Kutzelnigg *et al.*, 2005) and the effects of anatomical connectivity in the brain. Further evaluation of the relationship between chronic inflammation and the tract-specific effects on pathology using this novel imaging/histological strategy may provide valuable insight into the mechanism of tract-specific degeneration observed in this study. A better understanding of the underlying

mechanisms could offer the potential for targeted early therapeutic intervention to arrest the cascade of molecular processes leading to degeneration in distant but highly connected structures following focal insults.

Beyond evidence for the mechanisms of pathogenesis in multiple sclerosis, the findings presented here have a more direct diagnostic potential. The observation that cortical thickness derived from both histological and MRI data correlated significantly with neurodegenerative processes in deeper connected regions may be clinically useful in the diagnosis and assessment of patients with multiple sclerosis. Cortical atrophy is well described in multiple sclerosis, even in the early stages of the disease (Sailer *et al*., 2003; Dalton, 2004; Calabrese *et al*., 2007; Amato *et al*., 2012). Patterns of focal cortical atrophy have been reported previously in large imaging studies using standard diagnostic T_1-weighted MRI (Charil *et al*., 2007). Measures of cortical thickness could therefore provide a welcome biomarker beyond lesion load for the early assessment of diffuse disease activity to inform clinical decisions in multiple sclerosis, particularly as novel disease modifying therapeutic regimes may place an emphasis on early intervention (Goodin *et al*., 2009; Gilmore *et al*., 2010).

In addition to disease-specific findings, the data presented here suggest the persistence of the relationship between levels of myelination and corresponding diffusion-weighted MRI-derived tract fractional anisotropy and mean diffusivity in post-mortem fixed tissue (Fig. 5), supporting previous findings from studies of unfixed multiple sclerosis brain slices (Schmierer *et al*., 2007). This implies that underlying tissue microstructure continues to impact diffusion-weighted MRI metrics in fixed post-mortem brains, despite a global reduction in diffusion values and is of major relevance to future neuropathological study.

Unfixed tissue imaged rapidly after death is preferable for post-mortem scanning studies (Schmierer *et al*., 2007), but fixed samples are more readily available and convenient in terms of both storage and the maintenance of tissue integrity over time. However, the effect of post-mortem interval (time between death and fixation) and scan interval (time between fixation and scanning) on diffusion-weighted imaging and its reflection of tissue microstructure is controversial. Many argue that brain banks must address this issue if tissue is to be suitable for complex neuroimaging experiments (Grinberg *et al*., 2008). It has been demonstrated that post-mortem interval globally reduces diffusion-weighted MRI metrics in controlled rodent (D'Arceuil and de Crespigny, 2007), porcine (Widjaja *et al*., 2009) and donated human tissue (Kim *et al*., 2009), although scan interval does not have the same effect (Yong-Hing *et al*., 2005; Dyrby *et al*., 2010). Post-fixation degeneration has also been observed as extensive coarse hypointensities on MRI, but only after a period of >9 years in fixative (van Duijn *et al*., 2011). Further, acquisition protocols, data processing methods and pipelines optimized for use *in vivo* are unlikely to perform well post-mortem without careful adaptation (Pfefferbaum *et al*., 2004; Miller *et al*., 2011). These studies suggest that it is necessary to exercise caution when interpreting post-mortem data using assumptions from experience of *in vivo* imaging. However, with due care and the use of recent brain bank acquisitions, post-mortem scanning studies can offer novel structural insight on a global scale not seen in histological analysis alone.

Methodological limitations

The number of subjects in this study was relatively low due to the limited availability of samples and the extensive resources required for scanning and histological analysis. Control brains were not included; however, the degenerative markers studied are all well established in multiple sclerosis (Trapp and Nave, 2008), and given the study's aim to assess patterns of pathology across a range of patients with multiple sclerosis, the available resources were better directed at the study of a larger number of brains with a definitive multiple sclerosis diagnosis. Furthermore, given our investigation of intra-tract versus inter-tract patterns, individual subjects are effectively self-referencing. The *r*-values presented in the intra- versus inter-tract analysis were relatively low; however, the contrasting patterns of significance in correlations observed within and between the thalamo-cortical systems studied were in line with our predictions and suggest that our study was sufficiently well powered to detect meaningful relationships between measures. Similarly, the *r*-values presented in the correlations between diffusion-weighted imaging–MRI metrics and histological myelin quantification are reasonably low; this is expected to some extent as diffusion-weighted imaging–MRI metrics post-mortem are likely to be affected by factors in addition to myelination and other anatomical structures whose contribution is well defined *in vivo* (Beaulieu, 2002).

It is not possible to definitively prove the null hypothesis that there is no relationship between measures of cortical thickness in one tract projection system and degeneration in the white matter tract and thalamic nucleus of another. A lack of significant results might merely reflect the fact that our tests are insufficiently sensitive to detect a relationship. However, given the positive intra-tract relationships shown here, we believe that our tests are sufficiently sensitive to demonstrate a relationship where one exists and therefore are strongly indicative of an absence of inter-tract relationships.

Conclusion

This study demonstrates the presence of tract-specific patterns of pathology in multiple sclerosis, providing further evidence that diffuse neurodegeneration and non-lesional reductions in myelination previously associated with acute inflammation are linked in multiple sclerosis. Whilst the contribution of lesions to this pattern in diffuse pathology remains unclear, this finding offers the potential to guide further study of disease mechanisms for therapeutic intervention and highlights the utility of cortical thickness in the diagnosis or assessment of patients with multiple sclerosis. The detection of these patterns using post-mortem diffusion-weighted MRI and histology, along with the validation of diffusion-weighted MRI metrics in fixed brain tissue, demonstrate the relevance of this novel approach to future study in the field of neuropathology.

Acknowledgements

The authors thank Jessica Ward, Davina Ellis and Carolyn Sloan for assistance with clinical reporting, human tissue documentation and preparation of stained tissue. They further thank Timothy Carlisle for his assistance with cell profile counting, Drs Jesper Andersson and Tom Nichols for statistical advice and Dr MaryAnn Noonan for her assistance in magnetic resonance data acquisition. The authors acknowledge the support of the UK Multiple Sclerosis Brain Bank for supplying tissue samples and clinical information presented in this study.

Funding

This research was funded by The Multiple Sclerosis Society (to H.J.B.) and supported by the National Institute for Health Research (NIHR) Oxford Biomedical Research Centre (C.J.S/ H.J.B. and M.M.E.) based at Oxford University Hospitals Trust, Oxford University. The views expressed are those of the authors and not necessarily those of the NHS, the NIHR or the Department of Health. H.J.B. holds a Wellcome Trust Senior Research Fellowship; The Medical Research Council funded the MRI scanner used for post-mortem scanning.

Supplementary material

Supplementary material is available at *Brain* online.

References

Albert M, Antel J, Brück W, Stadelmann C. Extensive cortical remyelination in patients with chronic multiple sclerosis. Brain Pathol 2007; 17: 129–38.

Alper T, Barlow AJ, Gray RW, Kim MG, McLachlan RJ, Lamb J. Viscous, viscoelastic and dielectric properties of a perfluorinated polymer, Krytox 143-AB. J Chem Soc, Faraday Trans 2 1980; 76: 205–16.

Amato MP, Hakiki B, Goretti B, Rossi F, Stromillo ML, Giorgio A, et al. Association of MRI metrics and cognitive impairment in radiologically isolated syndromes. Neurology 2012; 78: 309–14.

Audoin B. Selective magnetization transfer ratio decrease in the visual cortex following optic neuritis. Brain 2006; 129: 1031–9.

Barbosa S, Blumhardt LD, Roberts N, Lock T, Edwards RH. Magnetic resonance relaxation time mapping in multiple sclerosis: normal appearing white matter and the "invisible" lesion load. Magn Reson Imaging 1994; 12: 33–42.

Beaulieu C. The basis of anisotropic water diffusion in the nervous system—a technical review. [Review]. NMR Biomed 2002; 15: 435–55.

Behrens TEJ, Woolrich MW, Jenkinson M, Johansen-Berg H, Nunes RG, Clare S, et al. Characterization and propagation of uncertainty in diffusion-weighted MR imaging. Magn Reson Med 2003a; 50: 1077–88.

Behrens TEJ, Johansen-Berg H, Woolrich MW, Smith SM, Wheeler-Kingshott CAM, Boulby PA, et al. Non-invasive mapping of connections between human thalamus and cortex using diffusion imaging. Nat Neurosci 2003b; 6: 750–7.

Behrens TEJ, Berg HJ, Jbabdi S, Rushworth MFS, Woolrich MW. Probabilistic diffusion tractography with multiple fibre orientations: What can we gain? NeuroImage 2007; 34: 144–55.

Bø L, Vedeler CA, Nyland HI, Trapp BD, Mørk SJ. Subpial demyelination in the cerebral cortex of multiple sclerosis patients. J Neuropathol Exp Neurol 2003; 62: 723–32.

Brownell B, Hughes JT. The distribution of plaques in the cerebrum in multiple sclerosis. J Neurol Neurosurg Psychiatry 1962; 25: 315–20.

Brück W, Bitsch A, Kolenda H, Brück Y, Stiefel M, Lassmann H. Inflammatory central nervous system demyelination: correlation of magnetic resonance imaging findings with lesion pathology. Ann Neurol 1997; 42: 783–93.

Calabrese M, Atzori M, Bernardi V, Morra A, Romualdi C, Rinaldi L, et al. Cortical atrophy is relevant in multiple sclerosis at clinical onset. J Neurol 2007; 254: 1212–20.

Caramanos Z, Francis SJ, Narayanan S, Lapierre Y, Arnold DL. Large, nonplateauing relationship between clinical disability and cerebral white matter lesion load in patients with multiple sclerosis. Arch Neurol 2012; 69: 89–95.

Carswell SR. Pathological anatomy.London: Longman, 1838.

Charcot J. Histologie de la sclerose en plaques. Gazette des hopitaux 1868; 41: 554–5.

Chard D, Griffin C, Parker G, Kapoor R. Brain atrophy in clinically early relapsing–remitting multiple sclerosis. Brain 2002; 125: 327–37.

Chard D, Miller D. Is multiple sclerosis a generalized disease of the central nervous system? An MRI perspective. [Review]. Curr Opin Neurol 2009; 22: 214–8.

Charil A, Dagher A, Lerch JP, Zijdenbos AP, Worsley KJ, Evans AC. Focal cortical atrophy in multiple sclerosis: Relation to lesion load and disability. NeuroImage 2007; 34: 509–17.

Ciccarelli O, Toosy AT, Hickman SJ, Parker GJM, Wheeler-Kingshott CAM, Miller DH. Optic radiation changes after optic neuritis detected by tractography-based group mapping. Hum Brain Mapp 2005; 25: 308–16.

Cifelli A, Arridge M, Jezzard P, Esiri MM, Palace J, Matthews PM. Thalamic neurodegeneration in multiple sclerosis. Ann Neurol 2002; 52: 650–3.

Compston A, Coles A. Multiple sclerosis. [Review]. Lancet 2008; 372: 1502–17.

Confavreux C, Vukusic S, Adeleine P. Early clinical predictors and progression of irreversible disability in multiple sclerosis: an amnesic process. Brain 2003; 126: 770–82.

D'Arceuil H, de Crespigny A. The effects of brain tissue decomposition on diffusion tensor imaging and tractography. NeuroImage 2007; 36: 64–8.

Dalton CM. Early development of multiple sclerosis is associated with progressive grey matter atrophy in patients presenting with clinically isolated syndromes. Brain 2004; 127: 1101–7.

De Groot CJ, Bergers E, Kamphorst W, Ravid R, Polman CH, Barkhof F, et al. Post-mortem MRI-guided sampling of multiple sclerosis brain lesions: increased yield of active demyelinating and (p)reactive lesions. Brain 2001; 124: 1635–45.

DeArmond SJ, Fusco MM, Dewey MM. Structure of the human brain: a photographic atlas. Oxford University Press; 1989.

DeLuca GC, Ebers GC, Esiri MM. Axonal loss in multiple sclerosis: a pathological survey of the corticospinal and sensory tracts. Brain 2004; 127: 1009–18.

DeLuca GC, Williams K, Evangelou N, Ebers GC, Esiri MM. The contribution of demyelination to axonal loss in multiple sclerosis. Brain 2006; 129: 1507–16.

Dineen RA, Vilisaar J, Hlinka J, Bradshaw CM, Morgan PS, Constantinescu CS, et al. Disconnection as a mechanism for cognitive dysfunction in multiple sclerosis. Brain 2009; 132: 239–49.

Dyrby TB, Baaré WFC, Alexander DC, Jelsing J, Garde E, Søgaard LV. An ex vivo imaging pipeline for producing high-quality and high-resolution diffusion-weighted imaging datasets. Hum Brain Mapp 2010; 32: 544–63.

Dua , et al. Atlas: Multiple Sclerosis Resources in the World 2008. Geneva: World Health Organisation; 2008.

Dziedzic T, Metz I, Dallenga T, König FB, Müller S, Stadelmann C, et al. Wallerian degeneration: a major component of early axonal pathology in multiple sclerosis. Brain Pathol 2010; 20: 976–85.

Evangelou N, Konz D, Esiri MM, Smith S, Palace J, Matthews PM. Regional axonal loss in the corpus callosum correlates with cerebral white matter lesion volume and distribution in multiple sclerosis. Brain 2000a; 123: 1845–9.

Evangelou N, Esiri M, Smith S. Quantitative pathological evidence for axonal loss in normal appearing white matter in multiple sclerosis. Ann Neurol 2000b; 47: 391–5.

Evangelou N, Konz D, Esiri MM, Smith S, Palace J, Matthews PM. Size-selective neuronal changes in the anterior optic pathways suggest a differential susceptibility to injury in multiple sclerosis. Brain 2001; 124: 1813–20.

Ferguson B, Matyszak MK, Esiri MM, Perry VH. Axonal damage in acute multiple sclerosis lesions. Brain 1997; 120: 393–9.

Fog T. Topographic distribution of plaques in the spinal cord in multiple sclerosis. Arch Neurol Psychiatry 1950; 63: 382.

Forster E, Mazzetti C, Pompili M. The effect of molecular structure on the properties of dielectric fluids. IEEE Trans Dielectr Electr Insul 1991; 26: 749–54.

Frazier JA, Chiu S, Breeze JL, Makris N, Lange N, Kennedy DN, et al. Structural brain magnetic resonance imaging of limbic and thalamic volumes in pediatric bipolar disorder. Am J Psychiatry 2005; 162: 1256–65.

Frischer JM, Bramow S, Dal-Bianco A, Lucchinetti CF, Rauschka H, Schmidbauer M, et al. The relation between inflammation and neurodegeneration in multiple sclerosis brains. Brain 2009; 132: 1175–89.

Geurts JJ, Barkhof F. Grey matter pathology in multiple sclerosis. [Review]. Lancet Neurol 2008; 7: 841–51.

Gilmore CP, Donaldson I, Bø L, Owens T, Lowe J, Evangelou N. Regional variations in the extent and pattern of grey matter demyelination in multiple sclerosis: a comparison between the cerebral cortex, cerebellar cortex, deep grey matter nuclei and the spinal cord. J Neurol Neurosurg Psychiatry 2009; 80: 182–7.

Gilmore C, Cottrell D, Scolding N, Wingerchuk D, Weinshenker B, Boggild M. A window of opportunity for no treatment in early multiple sclerosis? Mult Scler 2010; 16: 756–9.

Goldby F. A note on transneuronal atrophy in the human lateral geniculate body. J Neurol Neurosurg Psychiatry 1957; 20: 202–7.

Goodin D, Bates D. Review: Treatment of early multiple sclerosis: the value of treatment initiation after a first clinical episode. Mult Scler 2009; 15: 1175–82.

Gorgoraptis N, Wheeler-Kingshott CA, Jenkins TM, Altmann DR, Miller DH, Thompson AJ. Combining tractography and cortical measures to test system-specific hypotheses in multiple sclerosis. Mult Scler 2010; 16: 555–65.

Grinberg LT, Amaro E Jr, Teipel S, Santos dos DD, Pasqualucci CA, Leite REP, et al. Assessment of factors that confound MRI and neuropathological correlation of human postmortem brain tissue. Cell Tissue Banking 2008; 9: 195–203.

Henry RG, Shieh M, Okuda DT, Evangelista A, Gorno-Tempini ML, Pelletier D. Regional grey matter atrophy in clinically isolated syndromes at presentation. J Neurol Neurosurg Psychiatry 2008; 79: 1236–44.

Hirai T, Jones EG. A new parcellation of the human thalamus on the basis of histochemical staining. Brain Res 1989; 14: 1–34.

Hua K, Zhang J, Wakana S, Jiang H, Li X, Reich DS, et al. Tract probability maps in stereotaxic spaces: analyses of white matter anatomy and tract-specific quantification. NeuroImage 2008; 39: 336–47.

Johansen-Berg H, Behrens TEJ, Sillery E, Ciccarelli O, Thompson AJ, Smith SM, et al. Functional-anatomical validation and individual variation of diffusion tractography-based segmentation of the human thalamus. Cereb Cortex 2005; 15: 31–9.

Jones EG. Viewpoint: the core and matrix of thalamic organization. Neuroscience 1998; 85: 331–45.

Kim TH, Zollinger L, Shi XF, Rose J, Jeong EK. Diffusion tensor imaging of ex vivo cervical spinal cord specimens: the immediate and long-term effects of fixation on diffusivity. Anat Rec 2009; 292: 234–41.

Kremenchutzky M, Rice GPA, Baskerville J, Wingerchuk DM, Ebers GC. The natural history of multiple sclerosis: a geographically based study 9: observations on the progressive phase of the disease. Brain 2006; 129: 584–94.

Kutzelnigg A, Lucchinetti CF, Stadelmann C, Brück W, Rauschka H, Bergmann M, et al. Cortical demyelination and diffuse white matter injury in multiple sclerosis. Brain 2005; 128: 2705–12.

Lassmann H, Brück W, Lucchinetti C. Heterogeneity of multiple sclerosis pathogenesis: implications for diagnosis and therapy. Trends Mol Med 2001; 7: 115–21.

Leary SM, Davie CA, Parker GJ, Stevenson VL, Wang L, Barker GJ, et al. 1H magnetic resonance spectroscopy of normal appearing white matter in primary progressive multiple sclerosis. J Neurol 1999; 246: 1023–6.

Li DKB, Held U, Petkau J, Daumer M, Barkhof F, Fazekas F, et al. MRI T2 lesion burden in multiple sclerosis: a plateauing relationship with clinical disability. Neurology 2006; 66: 1384–9.

Lindberg RLP, De Groot CJA, Certa U, Ravid R, Hoffmann F, Kappos L, et al. Multiple sclerosis as a generalized CNS disease—comparative microarray analysis of normal appearing white matter and lesions in secondary progressive MS. J Neuroimmunol 2004; 152: 154–67.

Lopez-Diego RS, Weiner HL. Novel therapeutic strategies for multiple sclerosis—a multifaceted adversary. Nat Rev Drug Discov 2008; 7: 909–25.

Madigan MC. Preliminary morphometric study of tumor necrosis factor-alpha (TNF alpha)-induced rabbit optic neuropathy. Neurol Res 1996; 18: 233–6.

McAlpine D, Compston A. McAlpine's multiple sclerosis. 4th edn. London: Churchill Livingstone; 2005.

McDonald WI, Compston A, Edan G, Goodkin D, Hartung H-P, Lublin FD, et al. Recommended diagnostic criteria for multiple sclerosis: Guidelines from the international panel on the diagnosis of multiple sclerosis. Ann Neurol 2001; 50: 121–7.

Miller KL, Stagg CJ, Douaud G, Jbabdi S, Smith SM, Behrens TEJ, et al. Diffusion imaging of whole, post-mortem human brains on a clinical MRI scanner. NeuroImage 2011; 57: 167–81.

Morgen K, Sammer G, Courtney SM, Wolters T, Melchior H, Blecker CR, et al. Evidence for a direct association between cortical atrophy and cognitive impairment in relapsing–remitting MS. NeuroImage 2006; 30: 891–8.

Mistry N, Tallantyre EC, Dixon JE, Galazis N, Jaspan T, Morgan PS, et al. Focal multiple sclerosis lesions abound in 'normal appearing white matter'. Mult Scler 2011; 17: 1313–23.

Nichols T, Brett M, Andersson J, Wager T, Poline J-B. Valid conjunction inference with the minimum statistic. NeuroImage 2005; 25: 653–60.

Peterson JW, Bø L, Mörk S, Chang A, Trapp BD. Transected neurites, apoptotic neurons, and reduced inflammation in cortical multiple sclerosis lesions. Ann Neurol 2001; 50: 389–400.

Pfefferbaum A, Sullivan EV, Adalsteinsson E, Garrick T, Harper C. Postmortem MR imaging of formalin-fixed human brain. NeuroImage 2004; 21: 1585–95.

Polman CH, Reingold SC, Edan G, Filippi M, Hartung H-P, Kappos L, et al. Diagnostic criteria for multiple sclerosis: 2005 revisions to the "McDonald Criteria". Ann Neurol 2005; 58: 840–6.

Pomeroy IM, Jordan EK, Frank JA, Matthews PM, Esiri MM. Diffuse cortical atrophy in a marmoset model of multiple sclerosis. Neurosci Lett 2008; 437: 121–4.

Portaccio E, Amato MP, Bartolozzi ML, Zipoli V, Mortilla M, Guidi L, et al. Neocortical volume decrease in relapsing–remitting multiple sclerosis with mild cognitive impairment. J Neurol Sci 2006; 245: 195–9.

Reimer P, Parizel PM, Meaney JFM, Stichnoth FA. Clinical MR Imaging. Berlin: Springer Verlag; 2010.

Rocca MA, Pagani E, Absinta M, Valsasina P, Falini A, Scotti G, et al. Altered functional and structural connectivities in patients with MS: a 3-T study. Neurology 2007; 69: 2136–45.

Sailer M. Focal thinning of the cerebral cortex in multiple sclerosis. Brain 2003; 126: 1734–44.

Scalfari A, Neuhaus A, Degenhardt A, Rice GP, Muraro PA, Daumer M, et al. The natural history of multiple sclerosis: a geographically based study 10: relapses and long-term disability. Brain 2010; 133: 1914–29.

Schmierer K, Wheeler-Kingshott CAM, Boulby PA, Scaravilli F, Altmann DR, Barker GJ, et al. Diffusion tensor imaging of post-mortem multiple sclerosis brain. NeuroImage 2007; 35: 467–77.

Sepulcre J, Goñi J, Masdeu JC, Bejarano B, Vélez de Mendizábal N, Toledo JB, et al. Contribution of white matter lesions to gray matter atrophy in multiple sclerosis: evidence from voxel-based analysis of T1 lesions in the visual pathway. Arch Neurol 2009; 66: 173–9.

Shepherd TM, Flint JJ, Thelwall PE, Stanisz GJ, Mareci TH, Yachnis AT, et al. Postmortem interval alters the water relaxation and diffusion properties of rat nervous tissue: implications for MRI studies of human autopsy samples. NeuroImage 2009a; 44: 820–6.

Shepherd TM, Thelwall PE, Stanisz GJ, Blackband SJ. Aldehyde fixative solutions alter the water relaxation and diffusion properties of nervous tissue. Magn Reson Med 2009b; 62: 26–34.

Simon JH, Kinkel RP, Jacobs L, Bub L, Simonian N. A Wallerian degeneration pattern in patients at risk for MS. Neurology 2000; 54: 1155–60.

Smith SM, Jenkinson M, Woolrich MW, Beckmann CF, Behrens TEJ, Johansen-Berg H, et al. Advances in functional and structural MR image analysis and implementation as FSL. NeuroImage 2004; 23: S208–19.

Smith SM, Jenkinson M, Johansen-Berg H, Rueckert D, Nichols TE, Mackay CE, et al. Tract-based spatial statistics: voxelwise analysis of multi-subject diffusion data. NeuroImage 2006; 31: 1487–505.

Sormani MP, Rovaris M, Comi G, Filippi M. A reassessment of the plateauing relationship between T2 lesion load and disability in MS. Neurology 2009; 73: 1538–42.

Stadelmann C. Multiple sclerosis as a neurodegenerative disease: pathology, mechanisms and therapeutic implications. [Review]. Curr Opin Neurol 2011; 24: 224–9.

Stensaas SS, Eddington DK, Dobelle WH. The topography and variability of the primary visual cortex in man. J Neurosurg 1974; 40: 747–55.

Tallantyre EC, Bo L, Al-Rawashdeh O, Owens T, Polman CH, Lowe J, et al. Greater loss of axons in primary progressive multiple sclerosis plaques compared to secondary progressive disease. Brain 2009; 132: 1190–99.

Trapp BD, Nave K-A. Multiple sclerosis: an immune or neurodegenerative disorder? [Review]. Annu Rev Neurosci 2008; 31: 247–69.

van Duijn S, Nabuurs RJA, van Rooden S, Maat-Schieman MLC, van Duinen SG, van Buchem MA, et al. MRI artifacts in human brain tissue after prolonged formalin storage. Magn Reson Med 2011; 65: 1750–8.

Wegner C. Neocortical neuronal, synaptic, and glial loss in multiple sclerosis. Neurology 2006; 67: 960–7.

Weiner HL. The challenge of multiple sclerosis: How do we cure a chronic heterogeneous disease? Ann Neurol 2009; 65: 239–48.

Werring D, Brassat D, Droogan A, Clark C, Symms M, Barker G, et al. The pathogenesis of lesions and normal-appearing white matter changes in multiple sclerosis. Brain 2000; 123: 1667–76.

Wible CG, Shenton ME, Hokama H, Kikinis R, Jolesz FA, Metcalf D, et al. Prefrontal cortex and schizophrenia. A quantitative magnetic resonance imaging study. Arch Gen Psychiatry 1995; 52: 279–88.

Widjaja E, Wei X, Vidarsson L, Moineddin R, Macgowan CK, Nilsson D. Alteration of diffusion tensor parameters in postmortem brain. Magn Reson Imaging 2009; 27: 865–70.

Woolrich MW, Jbabdi S, Patenaude B, Chappell M, Makni S, Behrens T, et al. Bayesian analysis of neuroimaging data in FSL. NeuroImage 2009; 45: S173–86.

Wylezinska M, Cifelli A, Jezzard P, Palace J, Alecci M, Matthews PM. Thalamic neurodegeneration in relapsing-remitting multiple sclerosis. Neurology 2003; 60(12): 1949–1954.

Yong-Hing CJ, Obenaus A, Stryker R, Tong K, Sarty GE. Magnetic resonance imaging and mathematical modeling of progressive formalin fixation of the human brain. Magn Reson Med 2005; 54: 324–32.

Ziegler A, Mueller S. Analysis of freshly fixed and museum invertebrate specimens using high-resolution, high-throughput MRI. Methods Mol Biol 2011; 771: 633–51.